PHYSICAL REVIEW B VOLUME 39, NUMBER 16 1 JUNE 1989

First-principles calculation of crystal-field parameters in $Nd_2Fe_{14}B$

Xue-Fu Zhong* and W. Y. Ching
Department of Physics, University of Missouri-Kansas City, Kansas City, Missouri 64110

(Received 24 October 1988)

A new approach to calculating the crystal-field parameters in a perfect crystal based on real-space charge distribution from energy-band calculations is formulated. The contribution from the charges in the vicinity of the ion is evaluated numerically using a method of successive least-squares fitting. The contribution from other ion sites is approximated by a point-charge model, but with effective ionic charges obtained from the band calculation. The method is applied to the $Nd_2Fe_{14}B$ permanent magnet. The crystal-field parameters up to sixth order are calculated for the Nd site. The results are in good agreement with experimental analysis and are qualitatively different from the existing theoretical values based purely on a point-charge model.

I. INTRODUCTION

It is well known that the crystalline electric field (CEF) is of great importance in explaining almost all observed properties related to local electrons in a solid, such as magnetic resonance, magnetic structure, Mössbauer effect, etc. Although the formalism of CEF has been widely accepted, there is still a long-existing weak point in the theory pertaining to the calculation of crystal-field parameters (CFP). Historically, the first attempts were made by using a point-charge model (PCM),[1] which had attracted a great deal of interest because of its extraordinary simplicity. The PCM is by no means an exact theory, however, as it depends essentially on some arbitrary assumptions. In performing a PCM calculation for a specific system, one usually assigns a value for the effective ionic charge to each ion in the crystal without justification. The assignment of an effective ionic charge is subject only to some weak constraints such as electric charge neutrality;[2-4] hence the actual values of the effective charge used become quite arbitrary. Besides, the CFP's obtained from a PCM calculation are generally far from those expected from experimental analysis.[5] In some cases, the calculated values differ from the experimental ones by an order of magnitude.[6] It then becomes necessary to attempt other remedial procedures in order to bring the calculated values closer to the experimental ones. The simplest way is to introduce a factor of less than unity and call it a "screening factor." Burns suggested[7] screening factors of 0.5, 0.1, and 0.05 for the second-, fourth-, and sixth-order field terms of rare-earth ions, respectively, based on empirical data. But the "screening factors" are rather *ad hoc* entities and cannot be made universal. In spite of these drawbacks, PCM is still the prime method for calculating CFP. This is not desirable because it does not reflect the realistic charge-density distribution of an environment.

In the late sixties, one step further was taken in the study of the crystal field. The effects of covalent bonding between neighboring atoms on the CEF were investigated.[8,9] The energy-level splittings due to the crystal field were corrected by an inclusion of the covalency and charge overlap between local electrons and those in the outer shells. These studies had exposed some other shortcoming inherent to the PCM. In that approach, the environmental charges are always assumed to stay outside the region over which local electrons distribute, while the covalency itself means the environmental charges can penetrate into the local region. The covalency effect cannot be easily accounted for without some fundamental revision of the theory. These investigations did add something new to the theory of the crystal field in addition to the PCM, but there is still no systematic approach to calculate CFP realistically.

In 1979, Schmidt derived an expression for the direct Coulombic contribution of conduction electrons to the CEF in cubic rare-earth intermetallics.[10] He attempted a CEF calculation based on the charge distribution from the Bloch functions obtained from angumented plane-wave method (APW) band calculations. He even went further and calculated the effect of exchange interaction from the conduction electrons.[11] The discussion of exchange interaction is totally beyond the crystal-field formalism, because it does not have a static electric origin. Schmidt's attempt is important because it relates the CEF to the electronic energy bands in solids. The concept of CEF is physically a simple one, but to formulate it from first principles and put it into a computationally tractable form is a nontrivial task.

In recent years, band-structure calculations based on local-density-functional theory[12-14] have advanced to a highly sophisticated form so that many ground-state properties of simple solids can be accurately predicted.[15] The valence-electron charge-density distribution obtained from such calculations is usually of sufficient accuracy that they can be used to evaluate other properties from first principles. In this paper, we present a numerical scheme to calculate CFP of a $Nd_2Fe_{14}B$ permanent magnet based on realistic energy bands. Our approach differs from Schmidt's in that our numerical procedure is not limited to a specific method of band-structure calculation and is therefore universal. This is because the charge density of valence electrons can always be constructed from Bloch functions obtained by any method of band-structure calculation.

Our choice of $Nd_2Fe_{14}B$ as a prototype material for this study warrants some comment. Most investigations on the CEF focus on systems involving some impurity atoms in a host crystal such as transition-metal or rare-earth elements in a typical ionic solid. In such systems, the charge density is determined not only by the energy bands of the host crystal, but also the wave functions of the impurity states. Calculation of impurity states is, generally speaking, more difficult and less accurate than the band structure itself because of the highly localized nature of the impurity wave function and the complication involving impurity-impurity interaction. To avoid this difficulty, we confine ourselves to the study of CEF of a perfect crystal. On the other hand, the crystal field of the material must be experimentally well investigated such that a meaningful comparison with calculated CFP can be made.

In recent years, $Nd_2Fe_{14}B$ has received world-wide attention because of its extraordinary properties as a high-performance permanent magnet.[16] CEF in $Nd_2Fe_{14}B$ is considered to play a pivotal role in determining many of its unique magnetic properties. There are abundant theoretical evaluations[2–4,17–19] and experimental measurements[17,18,20–22] available with somewhat conflicting data among different groups. Lastly, Gu and Ching have recently reported the first realistic calculation of energy bands in $Nd_2Fe_{14}B$ and related compounds.[23] It is only natural to extend such investigations on $Nd_2Fe_{14}B$ to including a calculation of CEF using the wave functions from the band structure. Some preliminary results have been presented earlier.[24]

The organization of this paper is as follows: In Sec. II, we redefine the CFP so as to take into account the effect of penetration of environmental charges into the local region. In Sec. III, we outline the procedures for calculating the contributions from two different space regions: the first from the charges on other sites and the second from those in the local region surrounding the ion. The approximations involved in the numerical evaluation are discussed. In Sec. IV, we present our results of CFP at the Nd sites in $Nd_2Fe_{14}B$ and compare them with several experimental measurements and analysis. Some concluding remarks are given in the last section.

II. THE DEFINITION OF CRYSTAL-FIELD PARAMETERS

The CEF due to the environmental charges $\rho(\mathbf{R})$ as seen by a local electron is defined as[25]

$$V(r,\theta,\phi)=-\int \frac{e\rho(\mathbf{R})}{|\mathbf{r}-\mathbf{R}|}d\tau \ , \tag{1}$$

where (r,θ,ϕ) represent the coordinates of the local electron, and $\mathbf{R}$ describes the environment which gives rise to the field. The integral in (1) extends over the whole crystal and the environmental charge density is given by

$$\rho=\rho_c-\rho_a \ , \tag{2}$$

where ρ_c is the electric charge density in the crystal, whereas ρ_a is the charge density of the free atom corresponding to the ion at the site where the crystal field is taken.

In the usual treatment of crystal field theory, the Legendre polynomials are used to expand the factor $1/|\mathbf{r}-\mathbf{R}|$ and the environmental charges are always assumed to be outside the region where the local electrons distribute. With this assumption, the integration in (1) must be carried out under the condition $r<R$; thus the ambiguity in the Legendre polynomial expansion as to whether $r<R$ or $r>R$ is removed.[26] This leads to the following expression of crystal field:

$$V=B_{20}O_{20}+B_{22}O_{22}+B_{40}O_{40}+\cdots+B_{66}O_{66} \ . \tag{3}$$

The B_{20}, B_{22}, $B_{40}, \ldots, B_{66}$ are known as crystal field parameters and O_{nm}, the Stevens operators. In the PCM, the integral in (1) is reduced to a lattice summation and CFP can be explicitly written as follows:[1]

$$B_{nm}=\theta_j\langle r^n\rangle\gamma_{nm}A_{nm} \ . \tag{4}$$

Here θ_j is the Stevens factor, A_{nm} is a numerical factor which appears in front of the bracket of tesseral harmonics as defined in Ref. 1, so in our notation $\gamma_{nm}A_{nm}$ in (4) is equal to A_n^m in Ref. 1. $\langle r^n\rangle$ is the radial average of r^n, and

$$\gamma_{nm}=-\frac{4\pi e}{2n+1}\sum_{i=1}^{N}\frac{q_i}{R^{n+1}}Z_{nm}(\Theta_i,\Phi_i) \tag{5}$$

represents a lattice summation in which $Z_{nm}(\Theta,\Phi)$ stands for the tesseral harmonics, and q_i is the effective ionic charge on each site. The expression (4) is exactly the same as defined by Hutchings.[1]

Although it is difficult to give a precise description to the charge penetration in CEF theory as mentioned earlier, one can certainly refine the definition of CFP by partially taking this effect into account. This can be done without much complication if one starts with the distribution of the real environmental charge density. In principle, the charge penetration brings about changes both in Coulombic and exchange interactions. The latter is totally beyond the CEF theory and will not be addressed. For a proper modification of the Coulombic field, all we need to do is remove the condition $r<R$ in the expansion of (1). At first sight, this may lead to the invalidation of the definition of CFP, because of the ambiguity as to whether we should take r^n or r^{-n-1} to be averaged in Eq. (4). Here we shall suggest a simplification which allows us to evaluate the change in Coulombic field approximately while keeping the traditional formalism of CEF theory intact.

The local electrons, such as the f electrons in a rare-earth element, usually have a maximum in their radial distribution of charge density. We may introduce the concept of an average orbital radius $\langle r\rangle$ and approximate the charge density of local electrons as distributing on a spherical surface of radius $\langle r\rangle$. With this radius $\langle r\rangle$, the environmental charges are either outside or inside this sphere. Their Coulombic potential can be easily written as the sum of two different integrals. The CFP is now redefined by adding these two contributions, one from the charge density inside the sphere which represents the penetrating electrons, and the other from outside the sphere:

$$B_{nm} = \theta_j \langle r^n \rangle \gamma_{nm} A_{nm} \text{ if } R > \langle r \rangle \ , \tag{6}$$

$$= \theta_j \langle r^{-n-1} \rangle \gamma_{nm} A_{nm} \text{ if } R < \langle r \rangle \ , \tag{7}$$

$$\gamma_{nm} = -\frac{4\pi e}{2n+1} \int \frac{\rho(\mathbf{R})}{R^{n+1}} Z_{nm}(\Theta,\Phi) d\tau \text{ if } R > \langle r \rangle \ , \tag{8}$$

$$\gamma_{nm} = -\frac{4\pi e}{2n+1} \int R^n \rho(\mathbf{R}) Z_{nm}(\Theta,\Phi) d\tau \text{ if } R < \langle r \rangle \ , \tag{9}$$

where $d\tau = R^2 dR \sin\Theta d\Theta d\Phi$. For Nd in $Nd_2Fe_{14}B$, $\langle r \rangle$ is the average radius of the localized $4f$ electrons of the Nd atom. All the symbols used in this modified definition of CFP are the same as in the PCM.

Even though our assumption on the local electron distribution is oversimplified, we still expect the new definition to be an improvement over the original one. The original definition of CFP, which coincides with the integral (8), should account for the main part of the CFP because the integral covers a much larger space of the charge distribution, but the integral (9) does bring about appreciable addition in the region inside the sphere of local electrons. In the case of rare-earth element, the average radius $\langle r \rangle$ is actually very small (0.6187 Å in our calculation), the improvement by integral (9) is comparably unimportant. But for a strongly covalent system, the contribution from integral (9) will be much larger. However, in that case, some additional modifications may become necessary because the covalency affects not only the Coulombic interaction, but also the exchange interaction as well.

III. THE CALCULATION OF CRYSTAL-FIELD PARAMETERS

Based on the new definition of CFP described above, the main task for calculating the CFP boils down to the evaluation of the integral over the whole crystal. This is a rather formidable task even for a simple crystal, because the distribution of charge density in the real space has to be constructed from the wave functions obtained from band structure calculations. For $Nd_2Fe_{14}B$, the crystal structure is extremely complicated with 68 atoms of three different kinds in a low-symmetry tetragonal unit cell.[27] Numerical integration over the entire crystal is not practical and some approximations must be introduced to reduce the calculation to a manageable level.

Our first approximation is to reduce the domain of integration so as to make the calculation practical. The environmental charge is determined by the difference between the crystal and the free atom charge densities, of which the crystal charge density ρ_c is more difficult to determine accurately. In general, ρ_c consists of two parts: (1) all core charges including the nuclei, which can be considered as point charges; (2) valence electrons, the spatial distribution of which is determined by the energy band structure. It should be pointed out that ρ_c represents the whole electric charge distribution in a crystal. For metals, the valence electrons are also the conduction electrons. Once the ρ_c is properly constructed, the so called "screening" effect by the conduction electrons is automatically taken into account.

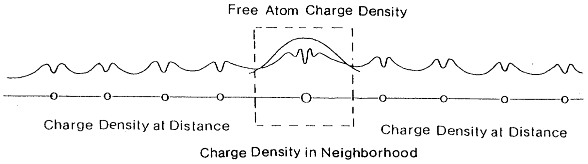

FIG. 1. Sketch of environmental charge distribution near the ion site and on the other sites.

In most crystals, the distribution of the valence charge around a core is almost spherically symmetric, especially when viewed from a distance. This suggests an idea that we should draw a distinction between the environmental charges which are in the vicinity of the ion under consideration and those on other sites. Figure 1 depicts schematically such a distinction. One can deal with these two parts of charge density separately by different arithmetics. The criterion for the division of these two types of charge will be made clear later. We shall now discuss the contributions from these two regions to CFP in more detail.

A. Contributions from charge density at distance (PCM calculation)

For charge density on other sites, we combine the core and valence electrons surrounding it into an effective ionic charge which is approximated as a point charge. This is valid because the potential of a spherically symmetric charge distribution is the same as that due to a point charge when viewed from a distance. This means the PCM is still applicable for this part of environmental charge. In order to assign a value to each of these point charges, we make use of the site-decomposed Mulliken charges as obtained from the band-structure calculation.[23] These numbers can be considered as the valence electrons at each lattice site. So the effective ionic charges in our calculation are

$$Q^* = Q_m + Q_c \ , \tag{10}$$

where Q_m represents the site-decomposed Mulliken charge and Q_c is the core charge including both core electrons and the nuclei. It must be emphasized that the effective ionic charges in (10) are realistic quantities obtained from first-principles band-structure calculation. This is in sharp contrast to the usual PCM calculations in which effective ionic charges are arbitrarily assumed parameters.

Table I lists the effective ionic charges on all sites in $Nd_2Fe_{14}B$, taken from Ref. 23. For comparison, the assumed values used in some PCM calculations[2,18] for $Nd_2Fe_{14}B$ are also listed. We have carried out a PCM calculation for $Nd_2Fe_{14}B$ using the effective ionic charges listed in Table I. The lattice summation extends to all ionic sites within a spherical region of radius 60 Å and a good convergence is obtained. The result of this calcula-

TABLE I. The effective ionic charges in $Nd_2Fe_{14}B$ used for CFP calculation using PCM.

	Nd	Nd	Fe	Fe	Fe	Fe	Fe	Fe	B
Site	f	g	e	c	j_1	j_2	k_1	k_2	f or g
Present[a]	1.65,	1.73	−0.14	0.73	−0.24	1.39	−0.47	−0.51	−2.38
Ref. 2	+3	+3	−9/14	−9/14	−9/14	−9/14	−9/14	−9/14	+3
Ref. 18	+3	+3	−0.5	−0.5	−0.5	−0.5	−0.5	−0.5	+1

[a] From band-structure calculation of Ref. 23.

TABLE II. Contribution to CFP from charge density at distance using a PCM.

(a) Second-order field terms in unit of K

	B_{20}		B_{22}	
Sites	f	g	f	g
Present work	6.54	9.08	−19.00	5.75
Ref. 2	−29.60	−28.34	32.61	−40.96
Ref. 18	−21.85	−18.54	14.37	−25.61

(b) Fourth-order field terms in unit of 10^{-2} K

		B_{40}	B_{42}	B_{44}
Present work	f	1.00	4.04	4.62
	g	1.06	−3.89	−4.21
Ref. 2	f	1.85	−4.69	−9.09
	g	1.72	3.64	6.20
Ref. 18	f	1.265	−1.902	−3.775
	g	1.103	−1.993	−3.537

(c) Sixth-order field terms in unit of 10^{-3} K

		B_{60}	B_{62}	B_{64}	B_{66}
Present work	f	0.06	−0.30	−0.49	−0.18
	g	0.05	−0.10	0.18	0.14
Ref. 2	f	−1.05		0.069	
	g	−0.923		−0.061	
Ref. 18	f	0.088	0.322	1.031	−3.549
	g	−0.075	−0.212	−0.927	0.530

TABLE III. Radial averages $\langle r^n \rangle$ for $4f$ atomic wave function of Nd.

	$\langle r^2 \rangle$	$\langle r^4 \rangle$	$\langle r^6 \rangle$	$\langle r^{-1} \rangle$	$\langle r^{-3} \rangle$	$\langle r^{-5} \rangle$
Present work	0.848 94	1.818 36	9.710 13	1.515 91	7.242 19	107.911 36
Ref. 32	1.040 25	2.122 98	6.595 47	1.366 99	5.450 78	61.697 36
Ref. 28	1.001	2.401	12.396		6.03	

tion represents, in our formalism, the partial contribution to CFP from the charge density on other sites. But in the usual PCM calculations, the lattice summation will constitute the total contribution to CFP from the environmental charges. It is, therefore, instructive to compare our partial results with some typical PCM calculations[2,18] for the same system. This is done in Table II where the CFP up to the sixth-order terms for both f and g sites of Nd ion are compared.

It should be pointed out that in the PCM calculation of Table II, we used a set of radial averages of r^2, r^4, r^6 which are somewhat different from those given by Ref. 28 (see Table III). The latter are more commonly used in the conventional CFP calculation. The reason for using different $\langle r^n \rangle$ values will be explained later. Here it suffices to say that in a test calculation, we used the same $\langle r^n \rangle$ values as in Ref. 28 and the same effective ionic charges as in Ref. 2 and had reproduced exactly the same results of Ref. 2.

As can be seen from Table II, the obvious features of our results in comparison with the existing ones are (1) the second order CFP, B_{20} and B_{22} which are the most important, are much smaller; (2) the signs of these two parameters are opposite to the existing results. These features are remarkable but not surprising, because the effective ionic charges we used were quite different. To understand these differences in more detail, we show in Fig. 2 the nearest neighbors of Nd in the basal plane of the tetragonal crystal[27] together with the assumed ionic charges. The other neighboring sites (Fe) are omitted because they are less important in determining the CFP on the Nd site. This is because all iron sites have much smaller effective ionic charges (see Table I) and are relatively further away from the Nd sites. It is clear from Fig. 2 that all positive ionic charges in our calculation are smaller than the values assumed in the existing PCM calculation. Of particular importance is the B site where the sign of the effective charge is opposite. We have B site as an anion based on the charge analysis from the band structure calculation,[23] while the existing calculations assume B to be a cation! The nature of ionic character of B in intermetallic compounds is a subject of considerable controversy. From the energy band calculation, the B 2s, B 2p states lie at about 6–10 eV below the Fermi level and this was confirmed by photoemission experiment.[29] The low-lying B 2s, B 2p states indicate that B must be an electron acceptor (anion) in $Nd_2Fe_{14}B$ instead of an electron donor as assumed in the existing PCM calculations for $Nd_2Fe_{14}B$.

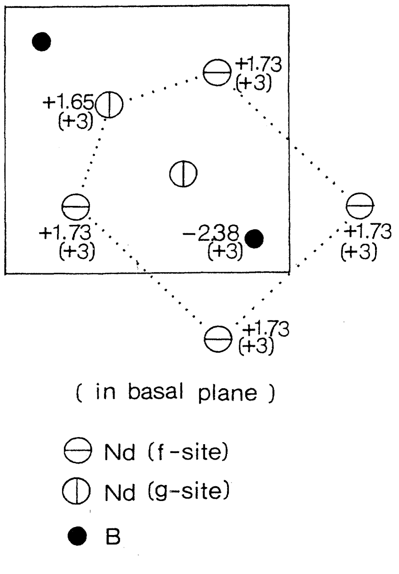

FIG. 2. The effective ionic charges of nearest neighbors of Nd in the basal plane of $Nd_2Fe_{14}B$. (Boron ion is an anion, not a cation).

B. Contributions from ρ in the neighborhood

The first approximation introduced in Sec. III A enables us to avoid the actual integration in core regions of all other sites where charge density oscillates sharply. However, the approximation cannot be applied to the charge density in the vicinity of the ion. On the contrary, the contribution from this part of the environmental charges to CFP is more cumbersome to evaluate. Because the region of interest is now in the neighborhood of the ion, the results will be sensitive to the detailed distribution of the charge density. We must carry out the integration as accurately as possible. Nevertheless, this time the integration domain is considerably reduced and only one core region at the center is left. For materials with a simple band structure, it might be possible to perform a three-dimensional integration by numerical method. But in the case of $Nd_2Fe_{14}B$, the Bloch wave functions are rather complicated and some further approximations are needed to simplify the calculation.

We first expand the charge distribution ρ in terms of tesseral harmonics:

$$\rho(\mathbf{R})=\rho_0(R)+\rho_{20}(R)Z_{20}(\Theta,\Phi)+\cdots+\rho_{66}(R)\mathbf{Z}_{66}(\Theta,\Phi)\,. \tag{11}$$

Here $\rho_0(R)$, $\rho_{20}(R),\ldots,\rho_{66}(R)$ are the "expansion coefficients" which are assumed to be spherically symmetric. (This means all angular dependence of the charge density is absorbed into the tesseral harmonics.) Inserting expression (11) into the expressions for γ_{nm} in Eq. (8) and Eq. (9), the integration for the angular part can be easily carried out due to the orthogonality of tesseral harmonics. We are left with only a one-dimensional integral in R which is much easier to compute numerically. Using this approach, the calculation of the contribution to CFP from the charge density in the vicinity of the on-site is considerably simplified.

The first term in the expansion (11), which is spherically symmetric, does not contribute to the crystal field. It only affects the Madelung potential of the crystal and therefore can be ignored. The question now is how to carry out the expansion (11). We have devised a numerical scheme which consists of successive applications of least-squares fitting of a sampled charge distribution in the real space. We start with a small sphere of radius R_0 around the ion and sampling $\rho(\mathbf{R})$ on it by numerically calculating $\rho(\mathbf{R})$ from the Bloch wave functions ψ_{nk} obtained from the energy band calculation:[23]

$$\rho(\mathbf{R})=\sum_{n,k}|\psi_{nk}(\mathbf{R})|^2 . \tag{12}$$

The summation over n is for all occupied bands and the summation over k space is approximated by a weighted sum of wave functions at 6 high-symmetry **k** points in the irreducible part of the Brillouin zone. A least squares fitting to the calculated data sample yields the "expansion coefficients" $\rho_0(R_0)$, $\rho_{20}(R_0), \ldots, \rho_{66}(R_0)$. The procedure is repeated on the next sphere with radius $R_1=R_0+\delta R$, where δR is a small increment determined by the desired accuracy of the calculation. By successive application of the same procedure, we obtain all the "expansion coefficients" $\rho_{nm}(R_i)$ as a function of the sphere radius R_i in a numerical form. R_i stops at a cutoff value R_c which defines the boundary between the charge density in the vicinity of the ion and those on other sites. Since Nd is a cation, whether it is on the f site or on the g site, there must be some net positive charges in its region. By sampling ρ on successive shells of spheres, we can evaluate the total charge in the neighborhood of the ion within the sphere of a given radius. As the radius becomes larger, there will be a maximum of accumulated positive charge at a certain radius after which the accumulated positive charge starts to decrease. This is illustrated in Fig. 3. We take the hypothesis that R_c should be the radius at which the accumulated positive charge is equal to the effective ionic charge obtained from the site decomposition of the Mulliken charges. The corresponding radius is then the ionic radius. We have determined R_c for Nd ion in our calculation to be 1.52 Å for both f and g sites and this value is clearly compatible with the usual ionic radius for rare earth elements. The cutoff radius R_c depends somewhat on the free-atom wave functions used to obtain ρ_a, but has little effect on the angular distribution of the charge density because the free-atom wave functions are spherically symmetric. This means that the major effect of different choices of free-atom wave function on the CFP calculation is the somewhat different values of R_c which defines the domain of integration for the contribution from the charge density in the vicinity of the on site. Since the integration must be done as accurately as possible, the choice of free-atom wave functions is a matter of considerable importance. At first sight, one might think of using some existing self-consistent atomic calculations, such as those by Hermann and Skillman,[30] Clementi and Toetti,[31] or Huzinaga.[32] There are some differences in charge densities derived from these calculations mainly because different orbitals were employed in the basis expansion. Generally speaking, calculations with Slater-type orbitals are more accurate. However, in the present case, the most important thing is to use atomic wave functions which are compatible with those used in the band-structure calculation. In Ref. 23, the Bloch functions were constructed from atomiclike wave functions by the method of contraction over a set of individual Gaussian-type orbitals.[33] In order to be consistent, we used the same set of Gaussian orbitals to contract our free atomic wave functions as in the orthogonalized linear combination of atomic orbitals (OLCAO) band structure calculation.[33] These atomic wave functions are usually more short-ranged than those from the usual atomic calculations. To keep the entire calculation internally consistent, we have also used the same contracted free atomic wave functions to evaluate the radial average of r^n or r^{-n-1} involved in the expressions (6) and (7) for CFP. The computation of radial averages is simple and straightforward but the results are slightly different from those of Freeman and Watson[28] which are more commonly used in crystal field calculation. Table III lists our radial averages and those from Ref. 28 for comparison.

The expansion (11) of $\rho(\mathbf{R})$ by means of successive least-squares fitting deserves some further comments. The method does not provide an exact expansion of charge density $\rho(\mathbf{R})$ in tesseral harmonics in analytic form, instead, all coefficients $\rho_{nm}(R)$ are obtained in the

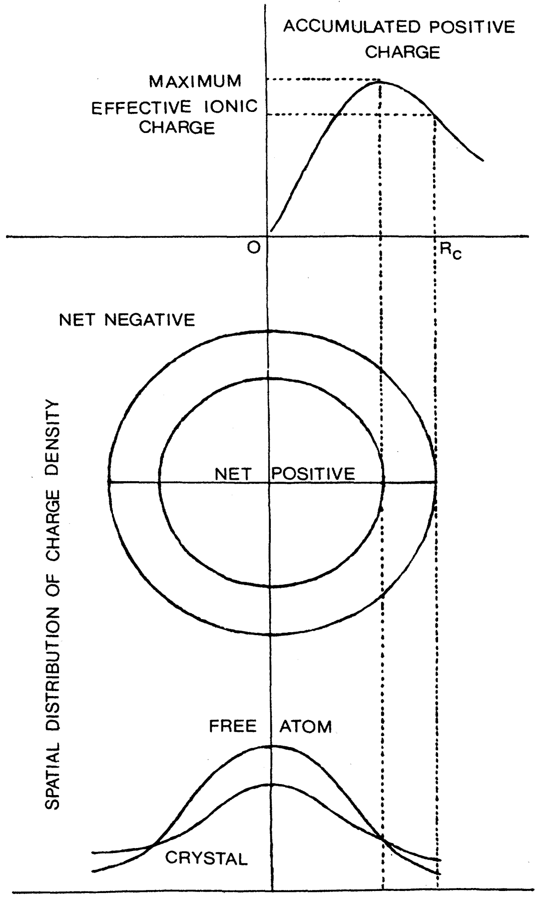

FIG. 3. Accumulated positive ionic charge as a function of radius of the sphere around a Nd site. Note the maximum occurs before the cutoff R_c where the accumulated positive ionic charge is equal to the effective ionic charge obtained from site decomposition of Mulliken charges.

TABLE IV. Contribution to CFP from charge density in the neighborhood as a function of sampling points.

(a) Second-order field terms in unit of K

Number of points	B_{20}		B_{22}	
	f site	g site	f site	g site
240	−10.41	−12.19	17.25	−4.46
308	−9.91	−11.67	17.48	−4.54
380	−10.24	−11.98	17.31	−4.48
462	−10.68	−11.89	18.15	−4.49

(b) Fourth-order field terms in unit of 10^{-2} K

Number of points	B_{40}		B_{42}		B_{44}	
	f site	g site	f site	g site	f site	g site
240	1.16	0.73	8.92	−2.45	−2.73	2.28
308	0.97	0.70	9.04	−2.41	−2.81	2.31
380	1.19	0.78	8.95	−2.37	−2.74	2.29
462	1.27	0.78	9.40	−2.46	−2.91	2.29

(c) Sixth-order field terms in unit of 10^{-3} K

Number of points	B_{60}		B_{62}		B_{64}		B_{66}	
	f site	g site	f site	g site	f site	g site	f site	g site
240	−26.88	−11.0	307.0	84.78	−22.11	−70.00	−19.98	−241.1
308	−28.63	−11.6	314.5	86.29	−22.96	−70.91	−20.45	−244.4
380	−19.67	−4.30	313.2	87.48	−22.52	−69.84	−20.16	−241.7
462	−17.62	−2.55	325.7	88.10	−24.20	−70.02	−21.25	−242.0

numerical form. $\rho(\mathbf{R})$ should be a continuous function of R, as should be all coefficients $\rho_{nm}(R)$. We have checked the continuity of $\rho_{nm}(R)$ and found it to be satisfactory for the whole range $0<R<R_c$.

It is important to realize that the charge distribution in the vicinity of the on-site ion is highly nonuniform. A large number of sampling points are usually required in the least squares fitting procedure in order to accurately mimic the angular dependence of the tesseral harmonics. On the other hand, the computational time increases rapidly as the number of sampling points N is increased. We have tested our CFP calculation on both f and g sites with increasing N per sphere and the results are listed in Table IV. It appears that a reasonably good convergency has been obtained for all CFP with N over 400. It is desirable to increase N even further for better convergence, but this will result in a tremendous increase in the computer time needed as to be impractical.

IV. RESULTS AND DISCUSSIONS

By adding the contributions from charge density in the vicinity of the ion and on the other sites, we arrive at the final results for CFP of Nd in $Nd_2Fe_{14}B$. For the first contribution, we take an average over all sampling tests listed in Table IV. This particular procedure has no special significance because the values from difference tests are very close. The CFP on both f and g sites up to the sixth-order terms are summarized in Table V.

The second-order field terms have been estimated by several experimental groups.[18,20] There are two kinds of measurement which are of particular interest: magnetization and Mössbauer measurements. From the analysis of the magnetic structure of $Nd_2Fe_{14}B$, Parker has obtained a value of −1.93 K for B_{20} on both f and g sites.[19] Recent work by Cadogan *et al.* gives a value of −2.2 K for the same parameter.[18] Besides, Radwanski and Franse, in a systematic analysis of crystal field of rare-earth–transition-metal–boron compounds, estimated B_{20} to be about $-2.0K$.[34] Thus the values for B_{20} from magnetic structure analysis are quite close to each other. On the other hand, data deduced from Mössbauer measurements estimate the B_{20} value to be -4.87 K and -4.94 K for f and g sites, respectively.[18] It should be noted that these numbers are the scaled values from those obtained in the Mössbauer study of $Gd_2Fe_{14}B$ by Boge

TABLE V. Final results of CFP of Nd sites in $Nd_2Fe_{14}B$.

(a) Second-order field terms in unit of K

Sites	B_{20}	B_{22}^c	B_{22}^s
f	−3.77	0.75	−1.45
g	−2.85	0.67	1.26

(b) Fourth-order field terms in unit of 10^{-2} K

Sites	B_{40}	B_{42}	B_{44}
f	2.15	5.04	1.40
g	1.81	6.31	−1.92

(c) Sixth-order field terms in unit of 10^{-3} K

Sites	B_{60}	B_{62}	B_{64}	B_{66}
f	−17.56	314.8	−23.44	−20.62
g	−2.50	86.56	−69.99	−242.2

et al.[21,22] Our calculated values for B_{20}, -3.77 K and -2.85 K for *f* and *g* sites, are in very good agreement with these experimental values. They are certainly much better than the existing PC calculation[2,3,18] which gave values a factor of 10 to 20 larger than the experimental estimates.

For the parameter B_{22}, the magnetization curve analysis gives values of ± 1.4 K and ± 4.3 K for *f* and *g* sites respectively[18], while the Mössbauer experiments give ± 3.21 K and ± 9.70 K for the corresponding sites.[18] Our calculated values of B_{22} for *f* and *g* sites are of the order 1 K, in rough agreement with the experimental values and are much smaller than those obtained from PCM calculation.[2,18]

The fourth-order field terms are generally less reliable than the second-order ones. Parker[20] gave an estimate of 0.025 K for B_{40} which is close to our calculated value of 0.0215 K. cadogan *et al.* estimate B_{40} to be 1.23 and 1.07×10^{-2} K and B_{44} to be -3.67 and 3.44×10^{-2} K for *f* and *g* sites, respectively,[18] from magnetization curve analysis. These are of the same order of magnitudes as our calculated values.

There are no experimental data on the sixth-order field terms, except Cadogan *et al.*[18] estimated B_{60} to be 1.25×10^{-3} K and B_{64} to be 18.94 and 7.22×10^{-3} K for both *f* and *g* sites, respectively. In fact, as pointed out by Schmidt,[10] the calculation for the sixth-order field terms using PCM is quite meaningless because the spatial patterns of the sixth-order tesseral harmonics are so complicated that their behavior can hardly be described by a limited number of neighboring sites (the number is limited by the convergence of the lattice summation). One can see from Tables IV and V that the contributions to the sixth-order field terms are mainly from the charge density in the vicinity of the on-site and they are of the same order of magnitude as the data extracted from experimental analysis. This clearly indicates that the PCM, which accounts only for the contribution from the charge density at sites away from the on site can lead to gross error in the sixth-order CFP.

The main evidence that our calculation of CFP in $Nd_2Fe_{14}B$ is successful is the good agreement on the second order field terms. We note that the signs of these terms in our final result are opposite to those in Table III, calculated with PCM, but using more realistic effective ionic charges. This implies that there is a competition between contributions to CFP from charge densities in the vicinity of the on site and those from other sites. In fact, the opposite results of Table III is mainly due to negative effective ionic charge of *B*, as can be seen from Fig. 2. By properly taking into account the effect of positive charges around the Nd cation, not only the signs of the CFP are reversed, but they also become much closer to the experimentally estimated values.

We need to emphasize at this point that all experimental values on CFP are subject to the limitations of the assumed theoretical models based on which the measured data are analyzed. These theoretical models are usually oversimplified. For example, it is always assumed[17,34] that some of the crystal-field terms can be totally ignored in the analysis of the experimental data. Nevertheless, we believe the order of the magnitude for CFP from the experimental analysis should be sufficiently accurate, especially for the second-order terms. What we try to emphasize here is that accurate determination of CFP from first-principles can facilitate experimental analysis such that more accurate estimations for CFP can be achieved.

The accuracy of our calculation depends mainly on two factors. One is related to the accuracy of the band structure from which the charge density distributon in crystal is derived. The other is the numerical accuracy involved in the evaluation of the CFP. It is prudent to discuss to what exent our results will be dependent on the calculated band structure of $Nd_2Fe_{14}B$. There are several aspects that need to be addressed.

First, any band-structure calculation always involves some sort of approximations. What we need is the electron wave functions that will provide a reasonably accurate description of the charge density in the crystal. The band-structure calculated by Gu and Ching can certainly be improved by iterating the crystal potential to full self-consistency and by including relativistic correction. But the major results, especially the site decomposition of the Mulliken charges, are not expected to change much by such refinements, since the calculated local spin magnetic moments on six different Fe sites in $Nd_2Fe_{14}B$ are in good agreement with experiments.[23] Therefore we believe the effective ionic charges used in our CFP calculation are reasonably accurate values. Another potential source of error has to do with the charge density in the core region. Since the band structure calculation of Ref. 22 is based on the OLCAO method[33] with a minimal basis set expanded in terms of Gaussian-type orbitals. The charge density distribution may be less accurate in the core regions than in other parts of the crystal. How much the nature of the basis orbitals may affect the CFP calculation is difficult to ascertain. Our calculation indicates that the contribution to the CFP is dominated by the charge density outside the average radius of local electrons. This is just what we have emphasized earlier in the modification of the definition of CFP. In fact the second integral (9) contributes only about 10% to the CFP. This is due to the fact that the 4*f* electrons in Nd are very localized and the covalency or charge penetration is relatively unimportant although not negligible. Thus, the specific form of orbitals used to form the basis functions in the band structure calculation will not significantly affect the calculated values for the CFP.

Second, the accuracy of the numerical procedures involved in our calculation can also be roughly estimated. In our final results for CFP, we have introduced an additional term B^c_{22} in the expansion (3). This term ought to be zero due to the symmetry of the field. Our calculation gives rise a small number of 0.71 K (average over *f* and *g* sites). This value comes only from the contribution due to the charge density in the vicinity of the on-site ion. Thus we may consider this value as a rough estimate of the numerical inaccuracy involved in the present calculation. For the fourth- and sixth-order field terms, the absolute error will be much smaller, but the relative error will be of the same level.

V. CONCLUSION

We have presented a new approach to calculate the CFP in a perfect crystal. This approach is based on the realistic charge density distribution in the crystal constructed from the Bloch functions obtained by accurate band-structure calculation. The contribution to the CFP is divided into two parts. One is from the ionic charge distribution on all sites other than the ionic site at which the CFP are evaluated and is obtained by using point charge model with the effective ionic charge at each site determined by the band-structure calculation. The other is from the charge distribution in the vicinity of the on site and is obtained by numerical integration. The contribution to CFP from these two parts may be of opposite signs, as in the case of Nd site in $Nd_2Fe_{14}B$, and their effective competition determines the final CFP values.

The new approach has been used to calculate the CFP at the Nd site of $Nd_2Fe_{14}B$, an important intermetallic compound noted for its high performance as a hard magnet. The calculated CFP values are in good agreement with experimentally determined values and are qualitatively different from those obtained by simple PCM calculations. The reasons for the poor results from the PCM are outlined and the importance of treating B as an anion is emphasized. Possible improvement on the accuracy of this type of new CFP calculation is also discussed.

Our new formalism of CFP calculation has not only clarified a vaguely defined concept, but also related the important parameters involved in such calculation to the more fundmental aspect of the theory of crystalline solids. Based on more accurately determined CFP from first principles, one can predict other interesting properties of materials where crystal field plays an important role. Furthermore, experimental data can now be analyzed more realisitcally without using arbitrary fitting parameters.

ACKNOWLEDGMENTS

This work is supported by the U.S. Department of Energy under Grant No. DE-FG02-84ER45170.

---

[*] On leave from Institute of Semiconductors, Chinese Academy of Sciences, Beijing, People's Republic of China.

[1] M. T. Hutching, Solid State Phys. **16**, 227 (1964).

[2] J. M. Cadogan and J. M. D. Coey, Phys. Rev. B **30**, 7326 (1984).

[3] H. Honma, M. Shimotomai, and M. Doyama, J. Magn. Magn. Mater. **52**, 399 (1985).

[4] S. Adam, G. Adam, and E. Burzo, J. Magn. Magn. Mater. **61**, 260 (1986).

[5] It is generally accepted that PCM works well only for purely ionic crystals.

[6] There are a great number of examples. Our system of $Nd_2Fe_{14}B$ is a rather typical one. The calculated CFP are 10 to 20 times larger than experimental estimates. See Sec. IV.

[7] G. Burns, J. Chem. Phys. **42**, 377 (1965).

[8] J. D. Axe and G. Burns, Phys. Rev. **152**, 331 (1966).

[9] R. E. Watson and A. J. Freeman, Phys. Rev. **156**, 251 (1967).

[10] D. Schmidt, J. Phys. F **9**, 1745 (1979).

[11] D. Schmidt, J. Phys. F **9**, 1759 (1979).

[12] B. I. Min, H. J. F. Jansen, T. Oguchi, and A. J. Freeman, J. Magn. Magn. Mater. **61**, 139 (1986).

[13] P. Hohenberg and W. Kohn, Phys. Rev. **136**, B864 (1964).

[14] W. Kohn and L. J. Sham, Phys. Rev. **140**, A1133 (1965).

[15] V. L. Moruzzi, J. F. Janak, and A. R. Williams, *Calculated Electronic Structure of Metals* (Pergamon, New York, 1978).

[16] See for details: Source Book on Neodymium-Iron-Boron Permanent Magnets, J. Capellen, K. A. Menzel, and K. A. Gschneidner, Jr., Rare Earth Information Center, Energy and Mineral Resources Research Institute, Iowa State University, 1986 (unpublished).

[17] D. Givord, H. S. Li, and R. Perrier de la Bathie, Solid State Commun. **51**, 857 (1984).

[18] J. M. Cadogan, J. P. Gavign, D. Givord, and H. S. Li, J. Phys. F **18**, 779 (1988).

[19] X. J. Lu, Y. Xu, G. L. Yang, H. R. Zhai, and Y. L. Liu, in *Proceedings of 8th International Workshop on Rare Earth Magnet, Dayton, Ohio, 1985* (University of Dayton Press, Dayton, 1985).

[20] F. T. Parker, J. Appl. Phys. **61**, 2606 (1987).

[21] M. Boge, J. M. D. Coey, G. Czjzek, D. Givord, C. Jeandey, H. S. Li, and J. L. Oddou, Solid State Commun. **55**, 295 (1985).

[22] M. Boge, G. Czjzek, D. Givord, C. Jeandey, H. S. Li, and J. L. Oddou, J. Phys. F. **16**, L67 (1986).

[23] Z. Q. Gu and W. Y. Ching, Phys. Rev. B **36**, 8530 (1987).

[24] Xue-Fu Zhong and W. Y. Ching, J. Appl. Phys. **64**, 5574 (1988).

[25] J. S. Griffith, *Theory of Transition Metal Ions* (Cambridge University Press, New York, 1961), p. 199.

[26] See Ref. 25, p. 200.

[27] J. F. Herbst, J. J. Croat, F. E. Pinkerton, and W. B. Yelon, Phys. Rev. B **29**, 4176 (1984).

[28] A. J. Freeman and R. E. Watson, Phys. Rev. **127**, 2058 (1962).

[29] D. J. Sellmyer, M. A. Engelhardt, S. S. Jaswal, and A. J. Arko Phys. Rev. Lett. **60**, 2077 (1988).

[30] F. Hermann and S. Skillman, *Atomic Structure Calculation* (Prentice-Hall, New York, 1963).

[31] E. Clementi and C. Roetti, Atomic Data Nucl. Data Tables **14**, 177 (1974).

[32] S. Huzinaga, *Gaussian Basis Sets for Molecular Calculation* (Elsevier, New York, 1984).

[33] W. Y. Ching and Chun C. Lin, Phys. Rev. B **12**, 5536 (1975).

[34] R. J. Radwanski and J. J. M. Franse, Phys. Rev. B **36**, 8616 (1987).